Mobility and Fading: Two Sides of the Same Coin

Zhenhua Gong and Martin Haenggi
Department of Electrical Engineering
University of Notre Dame
Notre Dame, IN 46556, USA
{zgong,mhaenggi}@nd.edu

***Abstract*—In wireless networks, distance variations caused by node mobility generate fluctuations of the channel gains. Such fluctuations can be treated as another type of fading besides multi-path effects. In this paper, we characterize the interference statistics in mobile random networks by mapping the distance variations of mobile nodes to the channel gain fluctuations. Network performance is evaluated in terms of the outage probability. A nearest-interferer approximation is employed. This approximation provides a tight lower bound on the outage probability. Comparing to a static network, we show that the interference distribution does not change under high mobility and random walk models, but random waypoint mobility increases interference.**

I. Introduction

Multi-path fading models *e.g.*, the Rayleigh and Nakagami models have been frequently employed to characterize wireless channels, treating small-scale fading as a stochastic component. On the other hand, power decay with distance or large-scale path loss is typically modeled as a deterministic component of wireless channels, given that the locations of a transmitter and a receiver are known, or the location uncertainty compared to the transmission distance is negligible. However, macroscopic mobility, which generates macroscopic changes in the transmission distance, also induces fluctuations of the channel gains. Hence, it can be viewed as another source of fading in wireless environments, in addition to the multi-path effects.

Understanding this type of fading induced by mobility is essential to deal with random networks because nodes are mobile in many applications. In [1], a network of mobile nodes is mapped to a network of stationary nodes with dynamic links. Path loss and multi-path fading uncertainty are treated jointly for single-hop connectivity and broadcasting in [2]. Previous research has only considered the distance uncertainty in the analysis. Interference in mobile networks remains an open problem. However, interference is one of the main issues in wireless networks, since it often limits network performance. Closed-form results of the interference and signal to interference ratio (SIR) distributions in static random networks are available in [3]–[5]. To the best of our knowledge, no work has focused on the interference statistics in mobile random networks.

In this paper, we characterize the interference distribution in mobile networks. Interference randomness is mainly composed of multi-path fading, power control [4], and random MAC schemes [5]. Besides these three elements, mobility is a source of randomness as well. Several mobility models are considered in the paper: high mobility (HM), random walk (RW), and random waypoint (RWP) [6]. The outage probability is used as a performance metric. In order to get closed-form expressions of the interference distribution and the outage probability, we approximate the total interference by only considering the contribution of the nearest interferer to a receiver.

To illustrate how mobility and fading are related, we start with a simple motivating example. The received power is exponentially distributed if the channel is subject to the Rayleigh fading. As a consequence, the SNR is exponential, as well as the SIR for constant interference power I. Next, we consider an infinite Poisson network with node intensity λ. Nodes are highly mobile. Hence, a new realization of the homogeneous Poisson point process (PPP) is drawn in every time slot. At a receiver, if we only focus on the interference from its nearest neighbor, the SIR $\gamma = 1/I = R_1^{\alpha}$, where R_1 is the distance between the receiver and its nearest neighbor, and α is the path loss exponent. From [2], we have the pdf of R_1 as

$$f_{R_1}(r) = 2\lambda\pi r e^{-\lambda\pi r^2}, \qquad r \geqslant 0. \tag{1}$$

Evidently, the pdf of γ is given by

$$f_{\gamma}(x) = \delta\lambda\pi x^{\delta-1} e^{-\lambda\pi x^{\delta}}, \qquad x \geqslant 0, \tag{2}$$

where $\delta \triangleq \frac{2}{\alpha}$. γ follows a Weibull distribution. For $\delta = 1$, we obtain

$$f_{\gamma}(x) = \lambda\pi e^{-\lambda\pi x}, \tag{3}$$

which is an exponential distribution. Hence, the distance variation leads the receiver to have the same SIR distribution as in the Rayleigh fading case. In other words, the receiver observes fading effects through the wireless channels due to the macroscopic mobility. Hence, mobility can be treated as another source of fading dynamics. In this example, the fading is more severe, when $\delta < 1$.[1]

Based on this observation, we characterize the interference distribution in mobile networks in the rest of the paper by mapping the distance variations of mobile nodes to the received power fluctuations in wireless channels.

[1]Detailed discussion will be in Section III-B.

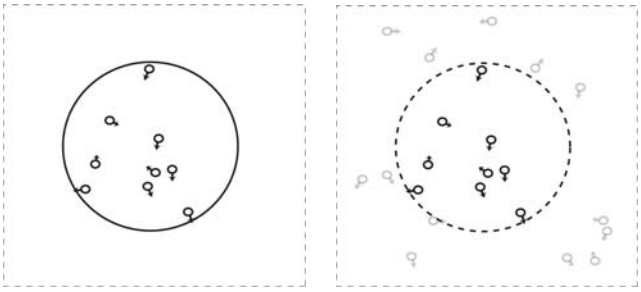

(a) Finite network (b) Infinite network

Figure 1. Illustrations of finite and infinite mobile networks. The small circles denote mobile nodes, and the arrows show the directions in which they will move in the next time slot. In (a), the nodes bounce back when they reach the boundary. In (b), all nodes move freely. Two categories of models are considered in (b). In an infinite model, all nodes are considered in analysis. In a cellular model, however, the nodes only inside a certain disk are considered (black nodes). The nodes outside the disk (gray nodes) belong to other cells, or they are neglected.

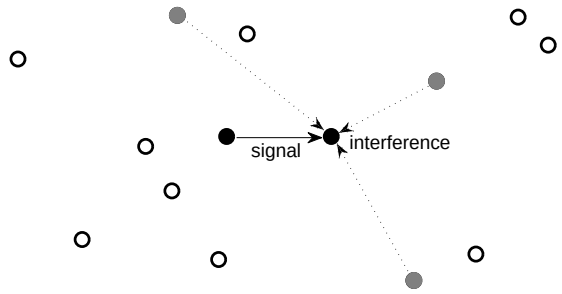

Figure 2. A network at one snapshot. A signal is transmitted from a transmitter to a receiver (solid black dots). Potential interfering nodes are randomly distributed and transmit with probability p. Nodes that are transmitting simultaneously (gray dots) cause interference to the receiver.

II. System and Mobility Models

A. Network and mobility models

We consider the link between a fixed transmitter and receiver pair in a wireless network. The distance between them is normalized to one. We set the origin o at the receiver. Initially (at time $t = 0$), other potential interfering transmitters follow a PPP $\hat{\Phi}$ on a domain $\mathbb{D}$ with intensity λ. In a finite network as shown in Figure 1 (left), $\mathbb{D} = B(o, R)$, where $B(o, R)$ is a 2-dimensional disk of radius R. The number of nodes M inside $B(o, R)$ is Poisson distributed with mean $\lambda\pi R^2$. In an infinite network as shown in Figure 1 (right), $\mathbb{D} = \mathbb{R}^2$.

After the initial placement, all nodes move independently of each other by updating their positions at the beginning of each time slot. In a finite network, the nodes bounce back when they reach the boundary so that M remains constant. In an infinite network, all nodes move freely. Two categories of models are often considered in this case. In an infinite model, all nodes are considered in the analysis. In a cellular model, however, the nodes only located in a certain disk are considered. The nodes outside the disk belong to other cells, or they are neglected.

The properties of three well accepted mobility models are listed as following:

1) High mobility (HM): The nodes are uniformly distributed in $\mathbb{D}$, and the realizations of the nodes placements in different time slots are independent.

2) Random walk (RW): A mobile node selects new direction and speed randomly and independently in each time slot. Hence, the spatial node distribution remains uniform [7].

3) Random waypoint (RWP): This model is restricted to a finite area. A node uniformly chooses a destination in the area and moves towards it with randomly selected speed. New direction and speed are chosen only after the node reaches the destination. Otherwise, it keeps the same direction and speed for several time slots. After a long running time, its spatial node distribution converges to a *non-uniform* steady distribution [8].

B. Channel model

The attenuation in the wireless channel is modeled as the product of a large-scale path gain component and a small-scale multi-path fading gain component. For the large-scale path gain, the received power decays with $r^{-\alpha}$, where r is the transmission distance. For the multi-path fading, we consider a deterministic model (*i.e.,* no fading) or the Rayleigh fading model in the desired link and the interference links. Following the notation in [9], we denote the fading state as a/b, where $a, b \in \{0, 1\}$ *e.g.,* 1/0. 1 represents the Rayleigh fading while 0 represents no fading. The first digit represents the channel of the desired link, and the second digit represents the channels of the interference links.

C. Channel access scheme

Slotted ALOHA is assumed as the channel access scheme. In every time slot t, where $t \in \mathbb{Z}$, each node determines whether to transmit or not independently with probability p.

D. Outage probability

The outage probability p_o is one of the fundamental performance metrics in wireless networks. In interference-limited channels, an outage occurs if the SIR at a receiver is lower than a certain threshold θ *i.e.,* $p_o = \mathbb{P}(\text{SIR} < \theta)$.

III. Interference in Uniformly Mobile Networks

A. Interference distribution without multi-path fading

In the analysis, we focus on the interference at the origin o. Figure 2 illustrates a transmitter and receiver pair in a network at one snapshot. A signal is transmitted from a transmitter to a receiver. Potential interfering nodes are randomly distributed and transmit with probability p. Nodes are highly mobile. Generally, the power received at the receiver from a transmitter is given by

$$P_{\mathrm{R}} = P_{\mathrm{T}} r^{-\alpha}, \tag{4}$$

where P_{T} is the transmit power. Without loss of generality, $P_{\mathrm{T}} = 1$. At time t, the total interference at the receiver is $I(t) = \sum_{x(t)\in\hat{\Phi}} T_x(t) \left\|x(t)\right\|^{-\alpha}$, where $T_x(t)$ is i.i.d.

Bernoulli with parameter p, and $\|\cdot\|$ is the Euclidean distance of a node to the origin. We set $\mathbb{D} = \mathbb{R}^2$. In the remainder of the paper, we are only interested in the interference distribution in a single time slot. Hence, we can drop the dependence on t. $I(t)$ can thus be simplified to

$$I = \sum_{x \in \hat{\Phi}} T_x \|x\|^{-\alpha}. \tag{5}$$

There are no closed-form pdf expressions of the interference[2], however, since the received power decays according to a power law, only considering the interference from the nearest interferer to the receiver provides a good approximation [4]. Therefore, we have the interference power approximately as

$$I \approx I_1 = R_1^{-\alpha}, \tag{6}$$

where $f_{R_1}(r)$ is in (1) with the interferer intensity $\lambda' = p\lambda$ due to the slotted ALOHA. Then, the pdf of I_1 is given by

$$f_{I_1}(x) = \delta p \lambda \pi x^{-\delta-1} e^{-p\lambda\pi x^{-\delta}}. \tag{7}$$

For higher dimensional cases *i.e.*, $d > 2$, (7) still holds, where $\delta = d/\alpha$.

If the RW model is used, the resulting spatial node distribution maintains uniform. All the results derived under the HM model are also valid for the RW model. Moreover, the same results can be obtained in finite networks and we omit the derivations.

B. The amount of fading

In a fading channel, the fading severity is quantified by *the amount of fading*, which is defined in [10] as

$$\mathrm{AF} = \frac{\mathrm{Var} S}{(\mathbb{E}S)^2},$$

where S is the signal power. Since we treat mobility as a source of fading and focus on the interference, we define a term $\mathrm{AF_M}$ to measure the fading severity induced by mobility, where

$$\mathrm{AF_M} = \frac{\mathrm{Var} I^{-1}}{(\mathbb{E}I^{-1})^2}.$$

Using (7), we obtain that for $\alpha > 1$,

$$\mathrm{AF_M}(\alpha) = \frac{\Gamma(1+\alpha)}{\Gamma(1+\alpha/2)^2} - 1. \tag{8}$$

We find that (8) increases with α or $2/\delta$. The fading is more severe at larger path loss exponent α. $\mathrm{AF_M}(2) = 1$, as expected from the example in the Section I.

C. Interference distribution with multi-path fading

When the interferers' channels are subject to multi-path fading, the interference power is

$$I_1 = h_1 R_1^{-\alpha}, \tag{9}$$

[2]In infinite networks, an exact expression is available only for $\alpha = 4$.

where h_1 is the multi-path fading coefficient. Defining $Y \triangleq R_1^{\alpha}$, we have

$$f_Y(y) = \delta p \lambda \pi y^{\delta-1} e^{-p\lambda\pi y^{\delta}}. \tag{10}$$

The pdf of I_1 is thus given by

$$f_{I_1}(z) = \int_0^{\infty} y f_{h_1}(yz) f_Y(y) \mathrm{d}y.$$

In the Rayleigh fading case, the cdf of I_1 is

$$F_{I_1}(z) = 1 - \int_0^{\infty} \delta p \lambda \pi y^{\delta-1} e^{-\left(p\lambda\pi y^{\delta} + zy\right)} \mathrm{d}y. \tag{11}$$

D. Lower bound on the outage probability

Once we obtain the interference or SIR distribution, the calculation for the outage probability is straightforward. First, if the desired channel is deterministic, a simple lower bound on the outage probability is derived using the nearest-interferer approximation

$$p_o^{0/a} = \mathbb{P}\left(\frac{1}{I} < \theta\right) \geqslant \mathbb{P}\left(\frac{1}{I_1} < \theta\right) = 1 - F_{I_1}(\theta^{-1}), \tag{12}$$

where we recall the notation $0/a$ defined in Section II-B and $a \in \{0, 1\}$.

Second, if the desired link is subject to the Rayleigh fading, the Laplace transform of the interference can be used to determine the outage probability [4], [5], whose lower bound is given by

$$p_o^{1/a} = 1 - \int_0^{\infty} e^{-h\theta} \mathrm{d}\mathbb{P}[I \leqslant h] = 1 - \mathcal{L}_I(\theta) \geqslant 1 - \mathcal{L}_{I_1}(\theta), \tag{13}$$

where $\mathcal{L}_I(\theta) = \int_0^{\infty} f_I(x) e^{-\theta x} \mathrm{d}x$ is the Laplace transform of the interference.

Under the RW model, the lower bounds on the outage probabilities in different fading states of the channels are plotted in Figure 3. The $p_o^{0/0}$ and $p_o^{1/0}$ curves are straightforward using (7). The $p_o^{0/1}$ and $p_o^{1/1}$ curves are calculated numerically using (11).

The simulation results of the exact outage probabilities in finite networks versus the corresponding lower bounds are shown in Figure 4, where the expected number of nodes $\mathbb{E}M = 10\pi \approx 31$. From the figure, we find that the nearest-interferer approximation provides a close approximation in terms of the outage probability. Furthermore, Multi-path fading is harmful to the link connections in mobile networks, when we compare the no fading case to the 1/1 fading case.

E. Exact expression of interference distribution

In infinite networks for $\alpha = 4$, we can derive an exact characterization of the interference instead of only considering the nearest-interferer dominance. We assume no fading in the interferers' channels. The interference distribution in static homogeneous Poisson networks, whose expression is in [3, (20)], can be extended to the distribution in mobile networks under the HM and RW models, since the spatial node distributions in both cases are uniform.

Figure 5 plots the comparison between the exact expressions of the outage probabilities and the corresponding lower bounds

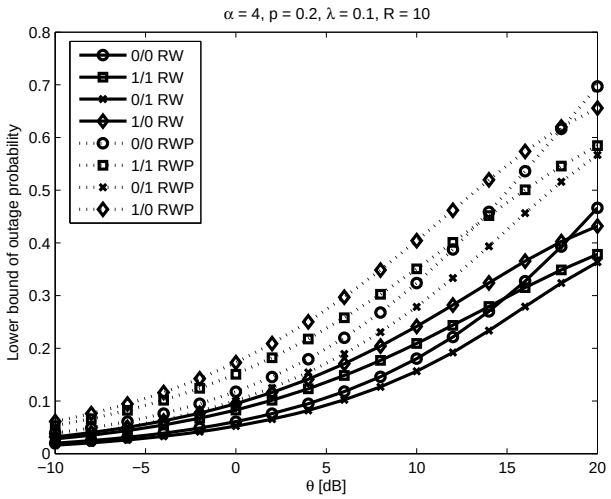

Figure 3. The lower bounds on the outage probabilities in different multi-path fading states of the channels, and under the RW and RWP models.

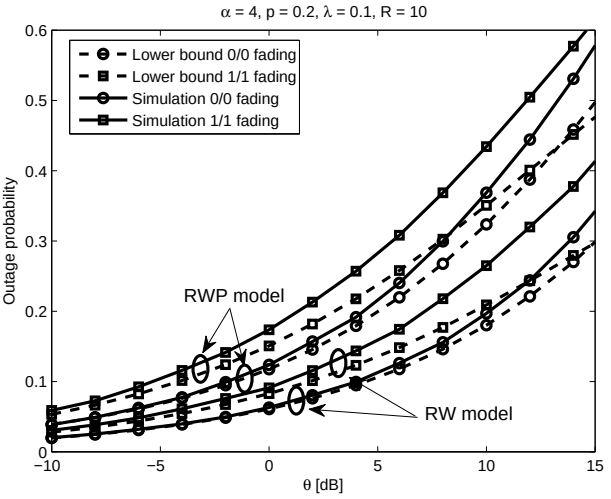

Figure 4. Simulation results versus the corresponding lower bounds for different fading states and different mobility models.

in infinite networks. The exact expressions are straightforward based on [3, (18) and (21)]. The bounds are tight, in particular of lower threshold regime, which is the regime of practical interest.

IV. Interference in Non-uniformly Mobile Networks

A. Interference in finite networks

In this section, we consider the RWP mobility. In finite networks, we have the node distance distribution from [8] as

$$f_L(r) = \frac{1}{R^2}\left(-\frac{4r^3}{R^2} + 4r\right). \tag{14}$$

Given a realization of the total number of nodes M, we have

$$\begin{aligned}\mathbb{P}\left(R_1 \leqslant r \mid M\right) &= 1-\left(1-F_L(r)\right)^M \\ &= 1-\left(1-\left(\frac{2r^2}{R^2}-\frac{r^4}{R^4}\right)\right)^M. \end{aligned} \tag{15}$$

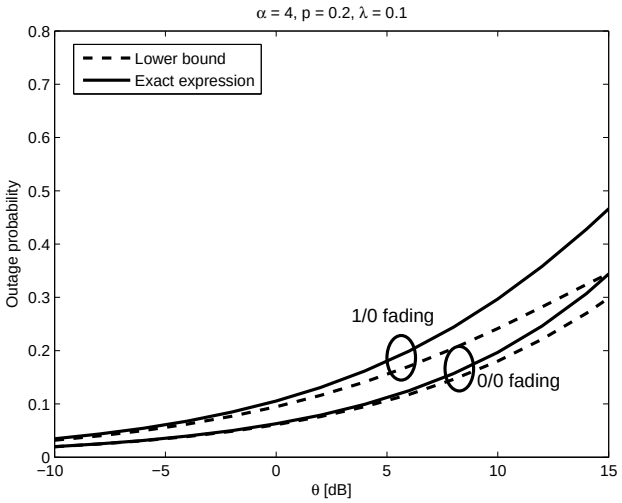

Figure 5. Comparison between the exact expressions of the outage probabilities and the lower bounds for different fading states in infinite networks. Nodes follow RW mobility.

Therefore, the pdf of R_1 with RWP nodes is given by

$$\begin{aligned} f_{R_1}(r) &= \frac{\mathrm{d}\mathbb{E}_M\left[\mathbb{P}\left(R_1 \leqslant r \,|M\right)\right]}{\mathrm{d}r} \\ &= p\lambda\pi\left(4r - 4\frac{r^3}{R^2}\right)e^{-p\lambda\pi\left(2r^2-\frac{r^4}{R^2}\right)}. \end{aligned} \tag{16}$$

Furthermore, using (6), (16), and taking the transformation of the random variable R_1, we obtain that the pdf of I_1 with RWP nodes is

$$f_{I_1}(x) = 2p\lambda\pi\delta\left(x^{-\delta-1} - \frac{x^{-2\delta-1}}{R^2}\right)e^{-p\lambda\pi\left(2x^{-\delta}-\frac{x^{-2\delta}}{R^2}\right)}. \tag{17}$$

The lower bounds on the outage probabilities and the simulation results are plotted in Figure 3 and Figure 4, respectively. Comparing to the RW model, we find that the RWP mobility increases interference. Moreover, the bounds under the RWP model are looser. Nodes are more likely to gather around the origin. Hence, more nodes besides the nearest one contribute to the interference.

B. Interference in infinite networks and issues of the mobility model

In infinite networks, the RWP model causes issues since it can not be properly defined. However, we can still get the exact characterization of the interference, if the distribution of node distance follows (14). The characteristic function of I, $\phi_I(\omega)$, is first calculated under a finite radius R. Then, we let $R \to \infty$. Since the mobility model itself can not be defined, such a result is not the interference characterization under the RWP model in infinite networks, but it provides an asymptotic expression as R gets large.

Recall that the total interference power is expressed in (5). After several steps of mathematical derivation, we obtain

$$\begin{aligned}\phi_I(\omega) &= \exp\left(\int_0^R \frac{4p\lambda\pi\left(rR^2-r^3\right)}{R^2}e^{j\omega r^{-\alpha}}\mathrm{d}r\right)\\ &\quad\cdot\exp\left(-p\lambda\pi R^2\right)\\ &= \exp\left(p\lambda\pi\alpha j\omega\int_0^R 2r^{-\alpha+1}e^{j\omega r^{-\alpha}}\mathrm{d}r\right)\\ &\quad\cdot\exp\left(-p\lambda\pi\alpha j\omega\int_0^R \frac{r^{-\alpha+3}}{R^2}e^{j\omega r^{-\alpha}}\mathrm{d}r\right).\end{aligned} \tag{18}$$

Our procedure here is similar to the one used in [3], but the node distribution is not uniform. Letting $R\to\infty$ and using the L'Hopital's rule, we obtain for $\alpha>2$ that

$$\lim_{R\to\infty}\int_0^R \frac{r^{-\alpha+3}}{R^2}e^{j\omega r^{-\alpha}}\mathrm{d}r = \lim_{R\to\infty}\frac{R^{-\alpha+2}e^{j\omega R^{-\alpha}}}{2}=0.$$

Hence, we have the second exponential factor in (18) as

$$\lim_{R\to\infty}\exp\left(-p\lambda\pi\alpha j\omega\int_0^R \frac{r^{-\alpha+3}}{R^2}e^{j\omega r^{-\alpha}}\mathrm{d}r\right)=1.$$

Therefore, following the derivations in [3], we have

$$\lim_{R\to\infty}\phi_I(\omega)=\exp\left(-2\pi p\lambda e^{-j\frac{\pi}{\alpha}}\omega^{\frac{2}{\alpha}}\Gamma(1-2/\alpha)\right). \tag{19}$$

Comparing (19) with [3, (18)], we obtain that in an asymptotically large area, the interference generated by RWP nodes is equivalent to the interference generated by RW or HM nodes with *doubled* node intensity ($\lambda'=2\lambda$). Without fading, the outage probability ($\alpha=4$) is given by

$$p_o^{0/0}=\mathbb{P}(I>\theta^{-1})=\mathrm{erf}\left(p\pi^{\frac{3}{2}}\sqrt{\theta}\lambda\right), \tag{20}$$

where $\mathrm{erf}(x)=2\int_0^x e^{-t^2}\mathrm{d}t/\sqrt{\pi}$ is the error function. If only the desired link is subject to the Rayleigh fading (1/0 fading), we replace $-j\omega$ in (19) to θ. Therefore, the outage probability is

$$p_o^{1/0}=1-\mathcal{L}_I(\theta)=1-e^{-2p\pi\lambda\theta^{2/\alpha}\Gamma(1-2/\alpha)}. \tag{21}$$

Obviously, the desired link has higher outage rate compared to the RW model.

Figure 6 shows the outage probabilities for RWP nodes with different radii R by simulations versus the asymptotic bound. The bound, which is the case for $R\to\infty$, is calculated using (20). As the figure depicts, the simulation curves become more close to the bound, when R gets larger. Hence, (20) can be viewed as the upper bound and the asymptotic expression of the outage probability for large R. The same result holds for (21).

V. Conclusions

In this paper, we have treated mobility from a fading perspective. Fluctuations of the path loss induced by mobility constitute another type of fading in wireless channels besides multi-path effects. To make the difference clear, we may speak of fading induced by microscopic mobility (multi-path fading) and fading induced by macroscopic mobility. Using this insight, we have characterized the interference distributions in mobile networks. The nearest-interferer approximation has been applied. It turns out that such approximation provides a tight lower bound on the outage probability. Moreover, we have shown that the RW and HM models do not affect the interference distribution compared to the static network. However, the RWP nodes generate more interference.

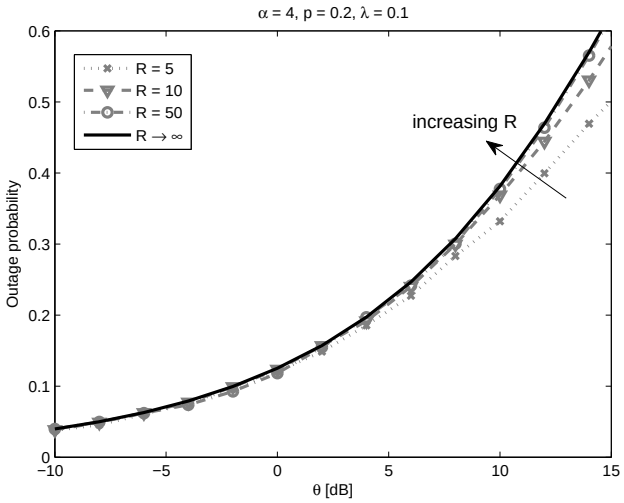

Figure 6. The outage probabilities under the RWP mobility with different radii R. Channel has no multi-path fading. The bound (solid-line curve) is calculated analytically using (20). Other curves with finite R are simulation results.

Acknowledgments

The partial support of NSF (grants CNS 04-47869, CCF 728763) and the DARPA/IPTO IT-MANET program (grant W911NF-07-1-0028) is gratefully acknowledged.

References

[1] Z. Kong and E. Yeh, "On the latency for information dissemination in mobile wireless networks," in *Proceedings of the 9th ACM international symposium on Mobile ad hoc networking and computing (MobiHoc)*, Hong Kong SAR, China, May 2008.

[2] M. Haenggi, "A Geometric Interpretation of Fading in Wireless Networks: Theory and Applications," *IEEE Trans. on Information Theory*, vol. 54, pp. 5500–5510, Dec 2008.

[3] E. Sousa and J. Silvester, "Optimum transmission ranges in a directsequence spread-spectrum multihop packet radio network," *IEEE Journal on Selected Areas in Communications*, vol. 8, pp. 762–771, Jun 1990.

[4] M. Haenggi and R. K. Ganti, *Interference in Large Wireless Networks*. Foundations and Trends in Networking (NOW Publishers), vol. 3, no. 2, pp. 127-248, 2008.

[5] F. Baccelli, B. Blaszczyszyn, and P. Muhlethaler, "An Aloha protocol for multihop mobile wireless networks," *IEEE Transactions on Information Theory*, vol. 52, no. 2, pp. 421–436, 2006.

[6] T. Camp, J. Boleng, and V. Davies, "A survey of mobility models for ad hoc network research Research," *Wireless Communications and Mobile Computing*, vol. 2, no. 5, pp. 483–502, 2002.

[7] S. Bandyopadhyay, E. J. Coyle, and T. Falck, "Stochastic properties of mobility models in mobile ad hoc networks," *IEEE Transactions on Mobile Computing*, vol. 6, no. 11, pp. 1218–1229, 2007.

[8] C. Bettstetter, G. Resta, and P. Santi, "The node distribution of the random waypoint mobility model for wireless ad hoc networks," *IEEE Transactions on Mobile Computing*, vol. 2, no. 3, pp. 257–269, 2003.

[9] M. Haenggi, "Outage, Local Throughput, and Capacity of Random Wireless Networks," *IEEE Transactions on Wireless Communications*, vol. 8, pp. 4350–4359, Aug 2009.

[10] U. Charash, "Reception through Nakagami fading multipath channels with random delays," *IEEE Transactions on Communications*, vol. 27, no. 4, pp. 657–670, 1979.